

# Vulnerability Analysis of China's Integrated Transportation Network Under Flooding: A Case Study of the July 20 Heavy Rain in Zhengzhou

Jingjing Kong<sup>1</sup>, Shuhe Lian<sup>1</sup>, Chao Zhang<sup>2</sup>

School of Civil Engineering, Shanghai Normal University, Shanghai, China<sup>1</sup>

E-mail: kongjingjing@shnu.edu.cn

School of Finance, Shanghai University of Finance and Economics, Shanghai, China<sup>2</sup>

E-mail: zhang.chao@sufe.edu.cn

## ABSTRACT

Frequent extreme rainfall and flooding increasingly threaten transportation system performance. This study constructs a China-wide integrated transportation network of expressways, railways, and aviation and develops a post-disaster passenger mode-switching model to assess network vulnerability based on passenger flow, travel delay, and on-time arrival rate. Using the July 20, 2021 Zhengzhou heavy rain as a case study, results show that modal complementarity limits functional degradation at the national scale, yielding relatively low overall vulnerability, with railways being the most vulnerable, followed by expressways and aviation. In flood-affected regions, however, vulnerability increases substantially, with aviation most affected, followed by expressways and railways. The findings provide quantitative support for flood risk management and resilience enhancement of integrated transportation systems.

**KEYWORDS:** comprehensive transportation system, vulnerability analysis, passenger flow, passenger delay time, passenger punctuality

## 1 INTRODUCTION

Transportation infrastructure, including highways, railways, and aviation systems, plays a critical role in supporting large-scale intercity passenger and freight mobility. In recent years, however, the increasing frequency and intensity of extreme weather events—particularly extreme rainfall and flooding—have posed growing threats to the functional safety and service continuity of transportation systems, leading to widespread disruptions and substantial economic and social losses. China has experienced multiple large-scale transportation disruptions caused by extreme weather, such as the 2008 southern China snow and ice disaster, the 2012 Beijing rainstorm, Typhoon Lekima in 2019, and the July 2021 extreme rainstorm in Zhengzhou, all of which resulted in expressway closures, railway suspensions, and large-scale flight cancellations.

Transportation system vulnerability is commonly defined as the sensitivity of a system to events that may cause a substantial reduction in service capacity (Berdica, 2002). Existing studies have extensively examined the vulnerability of individual transportation systems using network-based models, in which structural vulnerability is evaluated through topological indicators such as connectivity, centrality, clustering coefficient, and accessibility (Zhang et al., 2016; Kasturi and Amy, 2020; Yin and Wang, 2020; Sen et al., 2021). To better reflect real-world disruptions, a growing body of literature incorporates traffic flows and performance indicators—such as passenger volume, travel delay, and service disruption—into vulnerability analysis (Fang et al., 2016; Hong et al., 2015; Hong et al., 2019; Voltes-Dorta et al., 2017).

With increasing modal integration, transportation systems are interconnected through travelers' mode choice behavior, making integrated transportation networks more complex. Recent studies have examined complementary transportation systems, particularly coupled high-speed rail and aviation

networks, and shown that modal complementarity can partially mitigate vulnerability by providing alternative travel options (Ouyang et al., 2015; Li et al., 2019; Feng et al., 2021; Li and Rong, 2022). Nevertheless, existing research still pays limited attention to large-scale infrastructure failures caused by extreme weather and the resulting cascading disruptions across multiple transportation modes. Moreover, passenger behavioral responses—especially post-disaster mode switching—are often simplified or neglected.

To address these gaps, this study constructs a national integrated transportation network comprising expressway, railway, and aviation systems and develops a post-disaster passenger mode-switching model to capture interactions among transportation modes. Using the July 20, 2021 Zhengzhou extreme rainstorm as a case study, the proposed framework simulates the dynamic evolution of passenger flow, travel delay, and on-time arrival rate, thereby assessing the vulnerability of the national integrated transportation network from a functional perspective.

## 2 MODEL FORMULATION

### 2.1 Construction of the Integrated Transportation Infrastructure Network

To represent China’s integrated transportation system, a three-layer network is constructed based on expressways, railways, and aviation. The integrated transportation infrastructure network is defined as  $G = \{G_H, G_R, G_A\}$ , as illustrated in Figure 1, where nodes correspond to prefecture-level cities.

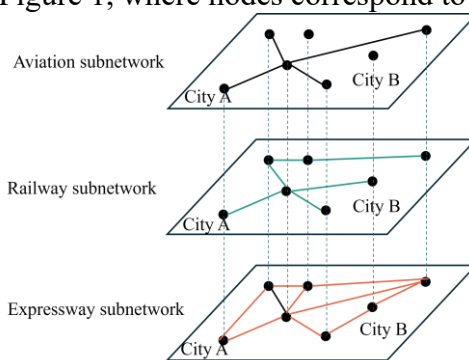


Figure 1: Schematic diagram of integrated transportation network

In the expressway subnetwork  $G_H$ , edges represent direct expressway connections between cities. The network is defined as  $G_H = \{N_H, E_H, L_H\}$ , where  $N_H$  denotes the set of cities connected by expressways,  $E_H$  the set of expressway links, and  $L_H$  the corresponding link lengths. Similarly, the railway subnetwork is defined as  $G_R = \{N_R, E_R, L_R\}$ , and the aviation subnetwork is defined as  $G_A = \{N_A, E_A, L_A\}$ .

To construct the national integrated transportation network, 293 prefecture-level cities with at least one of the three transportation modes are selected as nodes. City coordinate data and expressway and railway network data are obtained from the Amap (AMAP) open platform, while aviation network data are sourced from the OAG Analytics global aviation database. Owing to differences in infrastructure availability across cities, the expressway network contains 293 nodes and 625 edges, the railway network contains 275 nodes and 1,362 edges, and the aviation network contains 137 nodes and 1,949 edges.

### 2.2 Traffic Flow Modelling in Single-Layer Transportation Networks

To assess the impact of extreme weather on transportation service capacity, baseline passenger flows of expressway, railway, and aviation systems under normal conditions are first estimated.

For the expressway network, intercity coach schedules from the Checi platform (October 16, 2019) are used to identify direct services between city pairs. Passenger flows are allocated using an all-or-

nothing assignment along shortest paths, with vehicle type proportions determined based on national statistics.

For the railway network, train timetables released by the China Railway Customer Service Center (October 16, 2019) are used to construct intercity origin–destination pairs. For each pair, the train service with the fewest intermediate stops is selected as the representative flow. Given the short ticket inspection time, railway waiting time is not explicitly considered.

For the aviation network, only domestic prefecture-level flights are included. Flight schedules and passenger data are obtained from OAG Analytics (October 16, 2019), and a minimum pre-departure waiting time of 30 minutes is assumed in accordance with civil aviation regulations.

To ensure comparability across transportation modes, expressway vehicle flows, railway train capacities, and aircraft seating capacities are converted into passenger volumes using mode-specific assumptions. A standard passenger car is assumed to carry one passenger, train capacity corresponds to a conventional 16-car train set, and flight capacity equals the maximum seating capacity of the aircraft type. City-level origin–destination data are filtered and verified using Python. Due to data limitations, Hong Kong, Macao, and Taiwan are excluded from the analysis.

### 2.3 Passenger Mode Switching Model

Extreme weather may disrupt transportation services through expressway closures, railway station shutdowns, or airport closures, resulting in congestion and large numbers of stranded passengers. Assuming that passengers do not cancel their trips, they may switch travel modes to reach their destinations, thereby creating interactions among expressway, railway, and aviation networks. Under severe disruptions, travel time is assumed to be the primary criterion guiding passengers' mode choice.

Because railway and aviation services operate on fixed timetables, travel time after switching modes includes both waiting time for the next available service and in-vehicle travel time. Urban access time associated with mode switching is not considered, and waiting time is ignored when switching to expressways. The remaining travel time after switching modes is defined as the minimum sum of waiting time and in-vehicle travel time across all available modes:

$$T_{iD}^{change} = \min_{v \in \Omega} \{ T_{iD}^{wait, v} + T_{iD}^{trval, v} \} \quad (1)$$

where  $v$  denotes an alternative travel mode, and  $\Omega$  is the set of available modes, including expressway, railway, and aviation.  $T_{iD}^{wait, v}$  represents the required waiting time before boarding mode  $v$ , and  $T_{iD}^{trval, v}$  denotes the corresponding in-vehicle travel time to destination  $D$ .

When disruptions occur, passengers stranded at a network node (city  $i$ ) evaluate alternative modes based on the remaining travel time and switch only if sufficient capacity is available. If the selected mode exceeds its capacity constraint, another mode is considered. If all alternatives are capacity-constrained, the passenger remains stranded until service is restored. Passengers stranded on network links (e.g., expressway or railway segments) are assumed unable to switch modes and continue along the original route until infrastructure recovery. This process represents a flow reallocation mechanism across complementary transportation networks under capacity constraints.

### 2.4 Vulnerability Metrics for the National Integrated Transportation Network

From the perspective of transportation service performance, network vulnerability is evaluated using three key indicators: passenger flow, average travel delay, and on-time arrival rate. Vulnerability is quantified by the magnitude of changes in these indicators after extreme weather events, with larger deviations indicating higher vulnerability.

#### (1) Passenger Flow

Passenger flow at time  $t$  is defined as the total flow across expressway, railway, and aviation networks. Under normal conditions, flows follow shortest paths and published schedules. After extreme events, infrastructure disruptions such as road closures, train cancellations, and flight suspensions lead to congestion and flow redistribution across modes. Expressway flows are constrained by roadway capacity, while railway and aviation flows are limited by train and aircraft capacities. Passengers stranded on

network links remain on the original route until recovery, whereas those stranded at nodes may switch modes subject to capacity constraints, resulting in dynamic flow reallocation.

### (2) Average Travel Delay

Average travel delay captures the extent to which passengers fail to reach their destinations as planned. It is defined as the passenger-flow-weighted average delay across transportation modes. For expressways, delays arise from congestion and closures; for railways and aviation, delays result from disrupted or cancelled services. When mode switching is allowed, delays also include waiting time and remaining travel time after switching, capturing both direct disruption effects and indirect impacts of passenger reallocation.

### (3) On-Time Arrival Rate

The on-time arrival rate measures system reliability under extreme conditions. It is defined as the passenger-flow-weighted proportion of travelers who arrive within their planned travel time across all modes, accounting for both original and mode-switched trips. Lower on-time arrival rates indicate more severe disruptions and higher network vulnerability.

## 3 SIMULATION ANALYSIS

### 3.1 Scenario Construction: The July 20, 2021 Zhengzhou Rainstorm

From July 17 to July 23, 2021, Henan Province experienced an unprecedented extreme rainstorm, with Zhengzhou being the most severely affected city. The spatial distribution of cumulative precipitation in Henan province from July 17 to 21 is shown in Figure 2.

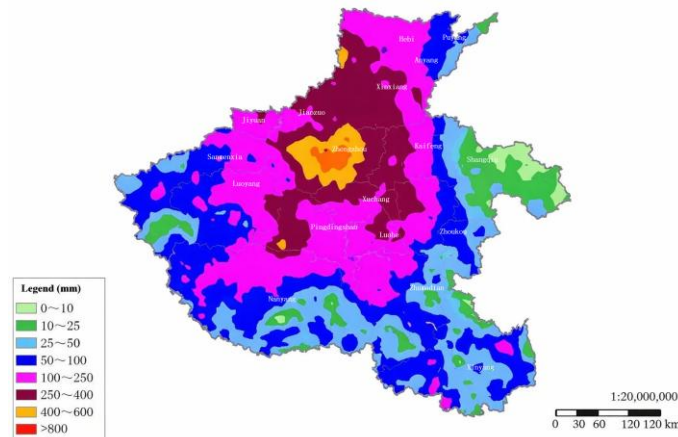


Figure 2: The spatial distribution of cumulative precipitation in Henan province from July 17 to 21

Record-breaking cumulative and hourly rainfall occurred during this period, causing widespread disruptions to transportation infrastructure, including expressway closures, railway service suspensions due to flooded tracks and damaged facilities, and large-scale flight cancellations at Zhengzhou Airport. Based on the observed impacts, a disaster scenario is constructed in which all expressway links, railway stations, and airports within the affected area are assumed to be closed, resulting in the suspension of corresponding services. Transportation facilities are assumed to operate in either a normal or failed state. The disaster onset time is set to 17:00 on July 20, corresponding to the peak hourly rainfall. Passenger flows are updated dynamically according to the proposed passenger flow and mode-switching models.

### 3.2 Vulnerability Analysis of the National Integrated Transportation Network

The simulation adopts a time step of 0.5 hours, yielding 48 time steps per day. Network performance is evaluated using three indicators—passenger flow, average travel delay, and on-time arrival rate—under both scenarios with and without passenger mode switching. To better demonstrate the post-disaster changes, the curve under normal conditions is also presented as a baseline for comparison. The normal or baseline state is defined as the routine operating condition of the integrated transport

system in the absence of extreme rainfall and flooding impacts. Under this condition, all relevant transport links and nodes are assumed to remain fully functional and accessible.

### (1) Passenger Flow

Figure 3 illustrates the temporal evolution of passenger flow in the national integrated transportation network. Under normal conditions, passenger flow exhibits a clear 24-hour periodic pattern. After the disaster, total passenger flow increases slightly regardless of whether passenger mode switching is considered, as some passengers are unable to reach their destinations and remain within the network.

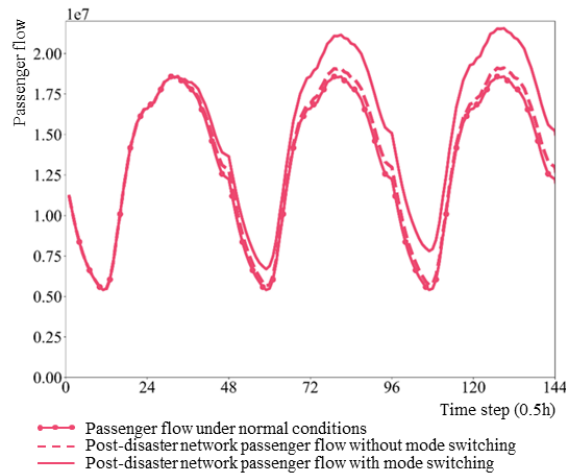


Figure 3: Passenger flow of China's integrated transportation network

To further examine the contribution of different transportation modes, Figure 4 presents passenger flow variations in expressway, railway, and aviation networks. After the disaster, expressway passenger flow increases, while railway and aviation passenger flows decline. When passenger mode switching is allowed, the increase in expressway flow becomes more pronounced, whereas the reductions in railway and aviation flows are larger. This indicates that passengers tend to switch from rail and air transport to expressways under prolonged service disruptions. In terms of flow variation, the expressway network exhibits the highest vulnerability, followed by the railway network, while the aviation network is the least affected.

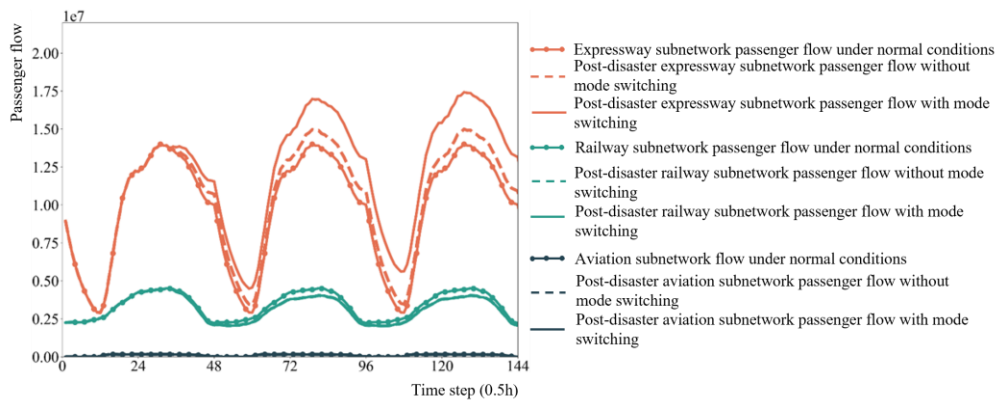


Figure 4: Passenger flow of subnetworks

### (2) Average Travel Delay

Figure 4 shows the average travel delay of the national integrated transportation network. After the disaster, average delay increases continuously, with a progressively rising growth rate. When passenger mode switching is allowed, average delay is consistently lower than in the no-switching scenario, indicating that mode switching can partially mitigate delay accumulation. Nevertheless, delays can still reach several times the normal average travel time, suggesting high vulnerability from a delay perspective.

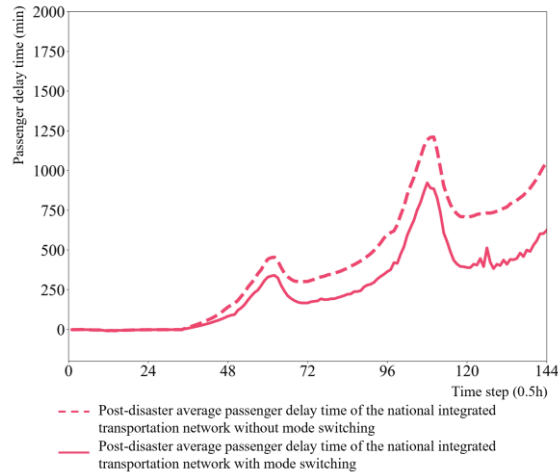


Figure 5: Average travel delay of China's integrated transportation network

Figure 6 further reports average travel delays by transportation mode. Without mode switching, railway delays are the largest, followed by aviation, while expressways experience the smallest delays. Allowing passenger mode switching substantially reduces delays in railway and aviation networks, but has limited impact on expressway delays due to capacity constraints. The two rapid growth phases of network-wide average delay are mainly driven by sharp increases in expressway and aviation delays.

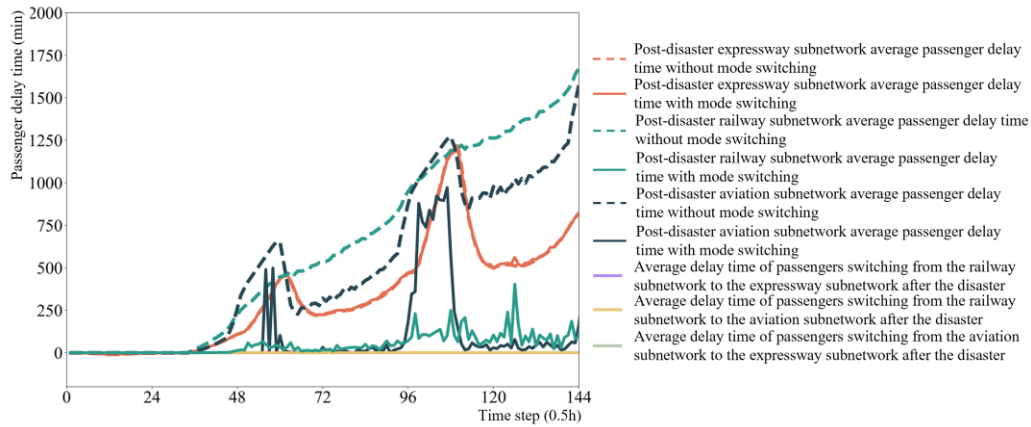


Figure 6: Average travel delay of subnetworks

### (3) On-Time Arrival Rate

Figure 7 presents the on-time arrival rate of the national integrated transportation network. After the disaster, the on-time arrival rate experiences several sharp declines, corresponding to the disaster onset and periods of rapidly increasing delays. When passenger mode switching is considered, the on-time arrival rate is lower than in the no-switching scenario, as most switching involves longer expressway travel times.

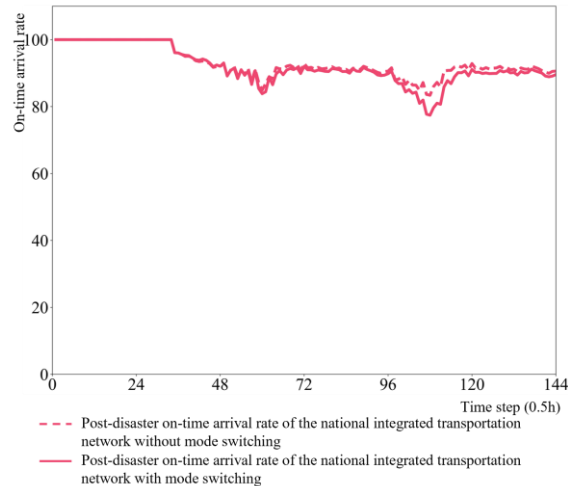


Figure 7: On-time arrival rate of China's integrated transportation network

Figure 8 reports on-time arrival rates for expressway, railway, and aviation networks. Aviation experiences the smallest decline, followed by expressways, while railways exhibit the largest reduction. These differences reflect the fixed schedules of rail and air services and the longer travel times associated with expressway substitution. The on-time arrival rates of railway and aviation networks are largely unaffected by whether mode switching is considered, as passengers originally using these modes cannot arrive on time once switching occurs.

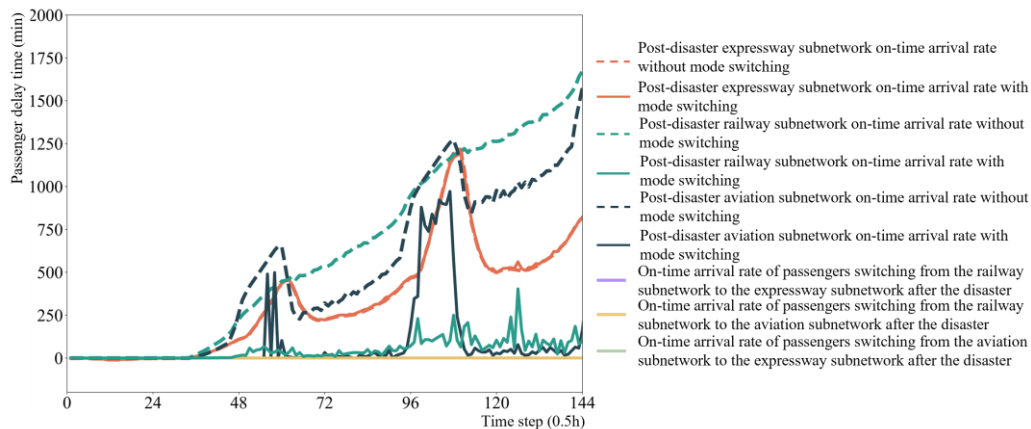


Figure 8: On-time arrival rate of subnetworks

Overall, the July 20 Zhengzhou rainstorm causes moderate disruptions to passenger flow and on-time arrival rates, but leads to substantial increases in travel delays. This indicates that the national integrated transportation network is more vulnerable from a delay perspective than from a flow or punctuality perspective. Allowing passenger mode switching reduces average travel delays but may further lower on-time arrival rates. From a mode-specific perspective, the expressway network exhibits the lowest vulnerability in terms of accessibility, followed by aviation, while the railway network shows the highest vulnerability when passenger flow, travel delay, and on-time arrival rate are jointly considered.

#### 4 CONCLUSION

This study proposes a post-disaster passenger mode-switching framework for a national integrated transportation network and evaluates functional vulnerability using the July 20, 2021 Zhengzhou rainstorm. Results indicate that China's transportation system exhibits low system-

level vulnerability due to strong modal complementarity, with railways being the most vulnerable, followed by expressways and aviation. The framework is extensible to other integrated transportation systems, while future work should incorporate behavioral responses, transfer times, and extreme congestion effects.

## REFERENCES

- Berdica K. (2002). An introduction to road vulnerability: What has been done, is done and should be done. *Transport Policy*, 9, 117–127.
- Fang S., Bian K. and Xie K. (2016). Vulnerability analysis of highway traffic networks using origin–destination tollgate data. *Proc. IEEE Int. Conf. Intell. Transp. Syst.*, 1–6.
- Feng X., He S., Chen X. et al. (2021). Mitigating the vulnerability of an air–high-speed railway transportation network: From the perspective of predisruption response. *Proc. Inst. Mech. Eng. Part O*, 235, 474–490.
- Hong L., Ouyang M., Peeta S. et al. (2015). Vulnerability assessment and mitigation for the Chinese railway system under floods. *Reliab. Eng. Syst. Saf.*, 137, 58–68.
- Hong L., Ye B., Yan H. et al. (2019). Spatiotemporal vulnerability analysis of railway systems with heterogeneous train flows. *Transp. Res. Part A*, 130, 725–744.
- Kasturi M. and Amy M.K. (2020). Vulnerability assessment of Alberta’s provincial highway network. *Transp. Res. Interdiscip. Perspect.*, 6, 100071.
- Li T., Rong L. and Yan K. (2019). Vulnerability analysis and critical area identification of public transport systems: A case of high-speed rail and air transport coupling in China. *Transp. Res. Part A*, 127, 55–70.
- Li T. and Rong L. (2022). Spatiotemporally complementary effect of high-speed rail network on robustness of aviation network. *Transp. Res. Part A*, 155, 95–114.
- Ouyang M., Pan Z. and He Y. (2015). Vulnerability analysis of complementary transportation systems with applications to railway and airline systems in China. *Reliab. Eng. Syst. Saf.*, 142, 248–257.
- Sen P., Dasgupta S., Chatterjee A. et al. (2021). Impacts of service features on vulnerability analysis of high-speed rail networks. *Transport Policy*, 110, 238–253.
- Voltes-Dorta A., Rodríguez-Déniz H. and Suau-Sánchez P. (2017). Vulnerability of the European air transport network to major airport closures from the perspective of passenger delays: Ranking the most critical airports. *Transp. Res. Part A*, 96, 119–145.
- Yin L. and Wang Y. (2020). Network characteristics and vulnerability analysis of Chinese railway networks under earthquake disasters. *Int. J. Geo-Inf.*, 9, 697.
- Zhang J., Hu F., Wang S. et al. (2016). Structural vulnerability and intervention of high-speed railway networks. *Physica A*, 462, 743–751.